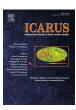


Contents lists available at ScienceDirect

Icarus

journal homepage: www.elsevier.com/locate/icarus



Thermal properties of Rhea's poles: Evidence for a meter-deep unconsolidated subsurface layer



C.J.A. Howett^{a,*}, J.R. Spencer^a, T. Hurford^b, A. Verbiscer^c, M. Segura^b

- ^a Southwest Research Institute, 1050 Walnut Street, Suite 300, Boulder, CO 80302, USA
- ^b NASA Goddard Spaceflight Center, Greenbelt, MD 20771, USA
- ^cDepartment of Astronomy, University of Virgina, Charlottesville, VA 22904, USA

ARTICLE INFO

Article history: Received 1 September 2015 Revised 22 February 2016 Accepted 23 February 2016 Available online 2 March 2016

Keywords: Satellites, surfaces Satellites, composition Saturn, satellites Infrared observations

ABSTRACT

Cassini's Composite Infrared Spectrometer (CIRS) observed both of Rhea's polar regions during a close (2000 km) flyby on 9th March 2013 during orbit 183. Rhea's southern pole was again observed during a more distant (51,000 km) flyby on 10th February 2015 during orbit 212. The results show Rhea's southern winter pole is one of the coldest places directly observed in our Solar System: surface temperatures of 25.4 ± 7.4 K and 24.7 ± 6.8 K are inferred from orbit 183 and 212 data, respectively. The surface temperature of the northern summer pole inferred from orbit 183 data is warmer: 66.6 ± 0.6 K. Assuming the surface thermophysical properties of the two polar regions are comparable then these temperatures can be considered a summer and winter seasonal temperature constraint for the polar region. Orbit 183 will provide solar longitude (L_S) coverage at 133° and 313° for the summer and winter poles respectively, while orbit 212 provides an additional winter temperature constraint at $L_{\rm S}$ 337°. Seasonal models with bolometric albedo values between 0.70 and 0.74 and thermal inertia values between 1 and $46\,\mathrm{J}\,\mathrm{m}^{-2}\,\mathrm{K}^{-1}\,\mathrm{s}^{-1/2}$ (otherwise known as MKS units) can provide adequate fits to these temperature constraints (assuming the winter temperature is an upper limit). Both these albedo and thermal inertia values agree within the uncertainties with those previously observed on both Rhea's leading and trailing hemispheres. Investigating the seasonal temperature change of Rhea's surface is particularly important, as the seasonal wave is sensitive to deeper surface temperatures (~tens of centimeters to meter depths) than the more commonly reported diurnal wave (typically less than a centimeter), the exact depth difference dependent upon the assumed surface properties. For example, if a surface porosity of 0.5 and thermal inertia of 25 MKS is assumed then the depth of the seasonal thermal wave is 76 cm, which is much deeper than the \sim 0.5 cm probed by diurnal studies of Rhea (Howett et al., 2010). The low thermal inertia derived here implies that Rhea's polar surfaces are highly porous even at great depths. Analysis of a CIRS focal plane $1 (10-600\,\mathrm{cm}^{-1})$ stare observation, taken during the orbit 183 encounter between 16:22:33 and 16:23:26 UT centered on 71.7°W, 58.7°S provides the first analysis of a thermal emissivity spectrum on Rhea. The results show a flat emissivity spectrum with negligible emissivity features. A few possible explanations exist for this flat emissivity spectrum, but the most likely for Rhea is that the surface is both highly porous and composed of small particles ($<\sim$ 50 μ m).

© 2016 Elsevier Inc. All rights reserved.

1. Introduction

On 9th March 2013 the Cassini spacecraft had a close (2000 km) encounter with Saturn's mid-sized icy satellite Rhea. The remote sensing instruments onboard Cassini viewed Rhea's southern winter hemisphere on approach and Rhea's northern summer hemisphere during departure at approximately nadir geometry. Thus, during one encounter high-spatial resolution observations were

obtained of both of Rhea's poles. Nearly two years later CIRS caught another glimpse of Rhea's southern pole, this time from further away ($51,000\,\mathrm{km}$) and at a high emission angle ($80-90^\circ$). To date these data sets provide the best coverage of Rhea's polar regions by CIRS, as they were taken at high-spatial resolution and at mostly low emission angles.

The Composite Infrared Spectrometer (CIRS) is one of Cassini's remote sensing instruments and was taking data during both of these Rhea encounters. It is from these data that the surface temperatures of Rhea's polar regions can be inferred, where a polar region is loosely defined as lying between the pole and 60°N/S. CIRS has three focal planes covering 10–1400 cm⁻¹

^{*} Corresponding author. Tel.: +1 720 240 0120; fax: +1 303 546 9687. E-mail address: howett@boulder.swri.edu (C.J.A. Howett).

Table 1Details of the encounter geometry during various significant periods of the March 9th 2013 and February 10th 2015 Cassini Rhea flybys. The sub-solar latitude was 18°N and 23.6°N during the entire observing period of the two flybys, respectively.

Date	Observation details	Start time (UT)	End time (UT)	Sub-spacecraft longitude (°W)	Sub-spacecraft latitude (deg.)	Range (km)	Sub-solar longitude (°W)	Spatial resolution of FP1 (km/pixel)
9th March 2013	FP1 map of Rhea's south polar region	15:58:14	16:22:23	126-128°W	64°S	63,203-77,329	11.012.4°W	246-301
9th March 2013	FP1 stare centered at 71.7°W and 58.7°S	16:22:33	16:23:26	128°W	64°S	62,621-63,110	12.412.5°W	244-246
9th March 2013	FP1 scan across Rhea's north polar region	18:20:11	18:25:14	197-251°W	56-73°N	4168-4678	18.8-19.1°W	16–18
10th February 2015	FP1 scan from equatorial latitudes to Rhea's south pole	07:38:00	07:55:00	304-310°W	24-27°S	49,744–51,773	183-184°W	194–202

(cf. Flasar et al., 2004). Focal plane 1 (FP1) covers $10\text{-}600\,\text{cm}^{-1}$ ($16.7\text{-}1000\,\mu\text{m}$), enabling the temperatures of even very cold surfaces to be determined ($<40\,\text{K}$). However, FP1's drawback is that it's made from a single circular detector, which has the lowest spatial resolution of CIRS' three focal planes ($3.9\,\text{mrad/pixel}$). The other focal planes (focal planes 3 and 4, known as FP3 and FP4) cover $600\text{-}1100\,\text{cm}^{-1}$ ($9.1\text{-}16.7\,\mu\text{m}$) and $1100\text{-}1400\,\text{cm}^{-1}$ ($7.1\text{-}9.1\,\mu\text{m}$) respectively, and are both 1×10 arrays of $0.273\,\text{mrad/pixel}$ detectors. These wavelength ranges make FP3 and FP4 sensitive to surfaces warmer than $65\,\text{K}$ and $110\,\text{K}$ respectively, thus making them only suitable for looking at the warmer daytime temperatures of satellites and Enceladus' active south polar terrain.

In 2010 Cassini's Ion Neutral Mass Spectrometer (INMS) discovered traces of molecular oxygen and carbon dioxide around Rhea (Teolis et al., 2010). Then evidence for a tenuous atmosphere around Dione was discovered using data collected in 2005 and 2010 by Cassini's Dual Technique Magnetometer (MAG) (Simon et al., 2011). The composition of Dione's tenuous atmosphere was later shown (using 2010 Cassini Plasma Spectrometer data) to include molecular oxygen (Tokar et al., 2012). Follow up observations showed that the gas concentrations were higher over the northern hemispheres of both satellites (Teolis et al., 2012), possibly due to seasonal variability. Since spring equinox in 2009 Rhea's (and Dione's) northern hemisphere has been warming, potentially causing volatiles previously trapped on its surface to sublimate. A surface capable of trapping the quantity of volatiles needed to produce the observed density of the exosphere must be both porous and cold (<50 K) (Teolis et al., 2010). Both of these requirements may be met in Rhea's polar regions. The presence of volatiles on the surface of Rhea, depending on their particle size and composition, could introduce observable emissivity variations into the CIRS spectrum. The previous study by Carvano et al. (2007) found no evidence of emissivity variations in the CIRS spectrum of Phoebe, Iapetus, Enceladus, Tethys or Hyperion, but did not consider Rhea or localized emissivity variations.

2. Data and analysis

2.1. Thermophysical property determination

CIRS' FP1 captures the majority of the blackbody emission thus providing the most robust surface temperature determination for both colder and warmer surfaces. Table 1 shows the CIRS FP1 data obtained both during the March 2013 and February 2015 flyby that are analyzed in this work. The low altitude of the March 2013 Cassini flyby provides high spatial resolution observations even with FP1 (16–359 km/pixel, see Table 1 for more information). Thus, during these two encounters FP1 has sufficient spatial resolution to determine polar temperatures and therefore only results from this focal plane will be discussed. During these observations the sub-solar latitude was low (18°N throughout the observation)

so the northern sunlit pole was observed at high phase (72°) . The more distant February 2015 observation had an FP1 spatial resolution between 194 and 202 km/pixel and viewed the southern pole at a high emission angle (>80°). Temperatures inferred from observations taken at high phase and high emission angles should be treated with a certain degree of caution because when rough terrain is viewed at these geometries non-representative surface regions are observed. For example during high phase observations a rough surface will create shadows that decrease the surface temperature observed by CIRS, which in turn would require a higher albedo and a lower thermal inertia to fit the observation. Whereas observations at high emission angles would preferentially observe high elevation regions (e.g. in this geometry equator-facing crater walls), the temperature of which may not be representative of the bulk surface temperature. These high elevation polar regions are probably warmer than their bulk surroundings since they will experience longer summer heating than the lower-lying and hence more shadowed neighboring terrain. Similar effects have already been observed on other icy satellites, for example Spencer (1987) analyzed Voyager 1 and 2's Infrared Interferometer Spectrometer and Radiometer (IRIS) observations of Callisto and found large variations of spectrum slope with emission angle at low solar elevation, which were attributed to the effect of surface topography. Such warmer temperatures require a lower albedo and higher thermal inertia to fit the observations.

For each CIRS spectrum, the best-fitting blackbody temperature emission curve is found using a downhill simplex method based on the work of Nelder and Mead (1965), as implemented in the IDL "amoeba" routine. Where observations overlap we calculate the mean spectral radiance, find the blackbody spectrum that fits this mean spectrum, and assume the corresponding blackbody temperature for the overlapping region. The spectral noise is converted to temperature noise using a two-step Monte Carlo technique (as detailed below). These surface temperatures of Rhea are then mapped, and the results are shown in Figs. 1 and 2 (south and north polar regions as observed in orbit 183) and Fig. 3 (south polar region as observed in orbit 212).

If we assume that surface thermophysical properties of both of Rhea's poles are the same, and that the temperatures of the fields of view that lie closest to the poles are comparable with those at the actual poles, then it is possible to use these observations to constrain Rhea's polar seasonal temperature variations. This is because both winter and summer temperature constraints are provided by these observations. There are of course potential problems with these assumptions. For example what if the thermophysical surface properties of each polar region greatly varies? That would mean that the surface temperatures close to the pole are in fact very different to those at the actual pole, and that the inferred temperatures are very dependent upon the size of the field of view (a problem since the FP1 field of view has a very different spatial resolution between the different polar

Download English Version:

https://daneshyari.com/en/article/8135266

Download Persian Version:

https://daneshyari.com/article/8135266

<u>Daneshyari.com</u>